



Cracking Assessment of Reinforced Concrete Slab Using Impact Hammer Test

Nuramieza Mohd Yazid¹, Nor Hayati Abd Ghafar^{1*}

¹ Faculty of Civil Engineering and Built Environment,
Universiti Tun Hussein Onn Malaysia, Batu Pahat, 86400, MALAYSIA

*Corresponding Author: noryati@uthm.edu.my

DOI: <https://doi.org/10.30880/jsmbe.2024.04.01.008>

Article Info

Received: 20 February 2024

Accepted: 27 May 2024

Available online: 30 June 2024

Keywords

Vibration, impact hammer, concrete

Abstract

Impact hammer test is a vibration-based monitoring method used to detect cracking or damage in concrete structures by observing the vibration behavior such as the natural frequency, mode shapes and damping ratio. Damage or cracks in the structure can cause structure failure. The ability to quickly perform maintenance, if necessary, depends on the ability to identify damage or cracks. Concrete cracking has traditionally been detected via vibration analysis utilizing the impact hammer test. The main objectives of this research were to determine the natural frequency of the cracked and uncracked reinforced concrete slabs and to determine the depth of the crack using the impact hammer test. Two samples of reinforced concrete slabs were constructed in the laboratory. The reinforced concrete slabs were designed as Grade 25 concrete. After 28 days, the impact hammer test was conducted on the uncracked slabs. After that, the slabs were subjected to a four-point bending test with loads of 3 kN, 6 kN, 12 kN and 15 kN. For each load increase, the impact hammer test and the crack mapping were performed. The natural frequency of the cracked and uncracked slabs was compared after that. The natural frequency of both Slab 1 and Slab 2 decreased after the slab was cracked compared to before cracked. The width of the crack was also determined by analyzing the wave acceleration from the impact hammer test. The outcome demonstrated that the wave's acceleration increased as it propagates through the crack region. The percentage difference in the waves' acceleration was calculated. The result was also compared with crack depth measurement from PUNDIT. The result showed that the location of the maximum crack width and crack depth was the same. It also justified that when the percentage difference of the acceleration decreased, the crack width increased. However, in previous studies, these findings had not been discussed yet. Therefore, further research needs to be done to understand the propagation of the wave on the cracked slab to validate the findings.

1. Introduction

Cracks can be defined as accidental discontinuities. Cracks typically result from localized material failure [1]. Cracking is a common problem that occurs in concrete structures. Cracking affects the durability of concrete, and the occurrence of cracking is influenced by many factors such as external stress, buckling, fatigue, physical process like freeze-thaw cycles, and chemical processes like alkali-silica reaction and corrosion [2]. Tiny cracks may result in inadequate serviceability whereas large cracks can cause structural failures. Early detection enables damage and potential failure to be avoided by taking preventive steps. Crack detection involves finding cracks in buildings using various processing techniques [3]. These days, vibration-based monitoring, also known as modal testing, has been widely used to detect any cracking on the structure at an early stage. The study of vibration-based monitoring or vibration-based damage detection involves recording and analyzing the vibration response of the monitored structure to assess structural damage and determine the state of structural health [4]. Differences in modal parameters which are natural frequency, mode shape, and damping ratio can all be assessed via vibration-based monitoring [5]. Impact hammer test and shaker test are the methods that can be applied in vibration-based monitoring to detect cracks in the concrete structure. However, this study will only focus on conducting impact hammer tests. Impact hammer is a quick damage assessment tool to detect cracks in concrete structures [6]. The impact hammer provided vibration and from the vibration analysis, a dynamic characteristic of the cracked concrete structure can be determined which are the natural frequencies, mode shapes and damping ratio. A vibration analysis using an impact hammer to detect cracking and to analyse modal parameters such as the natural frequency, mode shapes and damping ratio on the concrete structure has been put into practice a long time ago. The impact hammer test was a quite complicated test to be carried out due to the set-up. Many accelerometers were used as a sensor to record the vibration wave and it was essential to ensure all the accelerometers functioned well to avoid inaccurate data from being collected. Therefore, in this study, vibration-based monitoring through an impact hammer test was implemented to analyse the natural frequency of the reinforced concrete slab. The aim of this research is to determine the natural frequency of cracked and uncracked reinforced concrete slabs. This research was also conducted to evaluate the width of the crack by using an impact hammer test.

Vibration-based monitoring is a technique used for the assessment of cracks in concrete structures. Vibration-based monitoring is about using vibration data to locate damage to the structure [7]. Monitoring the state of the structure without changing it is a procedure known as Structural Health Monitoring (SHM) [8]. Vibration-based monitoring also has been a relevant method in determining structural safety since it can analyse the condition of the structure, including damage identification, categorization, and progressive development [9]. Vibration-based monitoring is also known as an alternative method to diagnose damage on concrete structures other than the visual inspection method which is performed manually. The vibration-based monitoring method is applied mostly in mechanical and aeronautic structures, civil structures and cultural heritage sites for example bridges, offshore construction, and power plants [10].

Vibration-based monitoring method identification of the damaged structure is based on the changes in dynamic characteristics which are the change in natural frequencies, mode shapes and damping ratios [11]. When there are changes in the mass, damping, and stiffness of the concrete structure caused by damage, vibration-based damage identification can be defined [12]. Modal attributes, such as natural frequencies, modal damping, and mode shapes, will change as a result of such modifications. Frequencies as well as mode shapes are the most important modal parameter to be observed in vibration-based monitoring. Generally, frequencies will drop if the structure has been damaged. Frequencies and mode shapes are observed together to pinpoint the damage location of the damage since mode shapes are more sensitive to damage [13]. The damaged structure will reduce the structure's local stiffness [14]. The decrement of the local stiffness will allow the vibration instrument to detect the change in natural frequencies, mode shapes and damping ratios. These vibration parameters can be analysed by the implementation of modal analysis testing using an impact hammer to produce vibration and the frequency of the vibration will be measured using accelerometers [6]. The application of vibration-based monitoring has been used widely to evaluate damage to concrete structures. It also can be used to conduct quality control and quality assessment of the concrete element. Vibration-based non-destructive test was applied to perform concrete quality control and identify concrete structural damage [15] and [16]. The damage detection on the dam structure is defined through the inspection of the difference in the natural frequencies, damping ratios and mode shapes. The application of a vibration-based monitoring technique can detect the damaged area in a multi-storey building according to the change of the natural frequencies and mode shapes [17]. Other than that, vibration-based monitoring also has been used in beams [18]. The difference in natural frequencies and mode shapes are obtained by the analytical and experimental model under six conditions of damages of the cantilever beams. Then, the location of the cracks in beams is determined by employing modal testing, the modal curvature and the modal flexibility method.

2. Impact Hammer Test

Modal testing, which involves monitoring structural health, is performed by utilizing an impact hammer as a vibration source. The hammer is impacted on the beam at a certain point and software was used to analyse the time response and Frequency-Response-Function (FRFs) of the beam [19]. The impact hammer test was conducted to evaluate the resonance frequency, damping ratio, and mode shape [15]. In the investigation of cracking on prestressed reinforced concrete and reinforced concrete beam using vibration-based monitoring, the prestressed reinforced concrete I-beam which is simply supported was subjected to bending load until the structural element formed a crack. The beam was hung by the flexible spring to allow the beam to be subjected to free vibration. Impact hammer test was conducted at a total of 27 different points and the response was recorded by the accelerometer. The Fast Fourier Transform (FFT) technique was used to extract the frequency produced from the impact hammer test. The testing process is the same for reinforced concrete beams as it is for prestressed reinforced concrete. According to the test's findings, reinforced concrete, and prestressed reinforced concrete, both had lower frequency values for concrete cracking. The first mode of vibration in the dynamic test on prestressed reinforced concrete beam varies linearly between one percent and five percent. The first vibration mode's frequency values for the reinforced concrete beam, meanwhile, range from 15 percent to 20 percent. Additionally, the dynamic response is affected by the reinforced concrete beam's nonlinear behavior, as evidenced by the decline in frequency values [15].

An impact test was applied to study its effectiveness in detecting damage in a reinforced concrete slab. A concrete slab of 3 meters by 1.35 meters was built for the experimental investigation in the lab [20]. A test grid of 42 points was plotted on the top and bottom surfaces of the slab. The accelerometers which were used to detect the change of frequencies were placed at the intersection of the test grid. After all the equipment was set up, the impact hammer test was conducted on the slab. The frequency response functions (FRFs) were analyzed using the software. The test was continued with the static test where the static load was applied on the slab to produce cracks. The impact hammer test was carried out once again to compare the frequency pattern between cracked and uncracked slabs. The results of the testing demonstrated that, according to the pattern of crack propagation with an increment of load, the gradient of the frequency along the decay increases as damage increases. It was different from other studies conducted on beams where the gradient of the frequency was reduced [20]. The assessment of damage on reinforced concrete flat slabs through the modal test was conducted to determine how damage affected the pattern of cracks and natural frequency in reinforced concrete slabs [9]. Two types of slabs with different dimensions and reinforcement ratios were constructed. Then, the test points were plotted on both surfaces of the slabs. After all the equipment was set, the modal test was conducted by using the impact hammer on both cracked and uncracked slabs. The test's findings revealed that both the slab's first natural frequencies had decreased. Then, the natural frequency of the slab that has a smaller longitudinal and transverse reinforcement ratio was almost steady from 40 percent to 70 percent of the ultimate load. Each slab's variations in natural frequency matched its pattern of cracking [9].

3. Materials and Methods

This section presents the materials and methods used to achieve the objectives of this study. All the materials and methods used were explained in detail in this section.

3.1 Materials

A reinforced concrete slab was constructed in the laboratory. The slab had dimensions of 1.6 m in length, 0.6 m in width and 0.1 m in thickness with a concrete cover of 2.5 cm. The reinforcement steel mesh provided was 5 mm in diameter with 200 mm spacing. The reinforced concrete slab was designed to be Grade 25. Figure 1 shows the reinforcement steel mesh used in the construction of the slabs and Figure 2 shows the reinforced concrete slab after the formwork was removed.

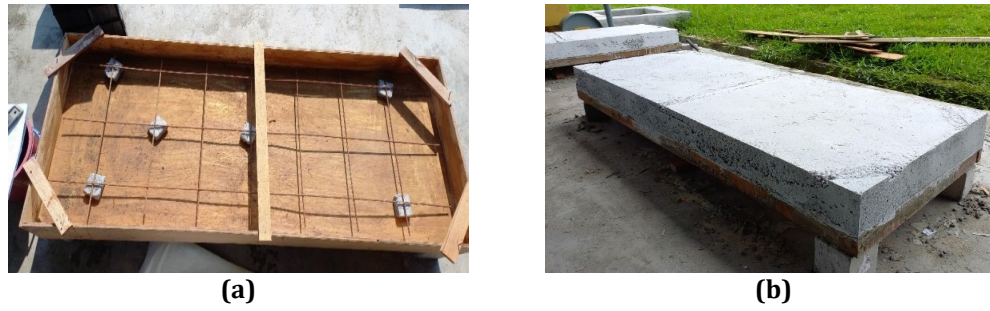


Fig. 1 Sample of slab (a) Reinforcement steel mesh; (b) Reinforced concrete slab

3.2 Methods

After 28 days, when the concrete reached a compressive strength of 25 MPa, the gridlines were plotted on the slab along the length and the width of the slab as shown in Figure 2 (a). The function of drawing the grid line was to create a point where the accelerometers were placed as shown in Figure 2 (b) and Figure 3 shows the schematic diagram of the location of accelerometers.



Fig. 2 Sample of slab (a) Gridlines on the slab; (b) Location of the accelerometer

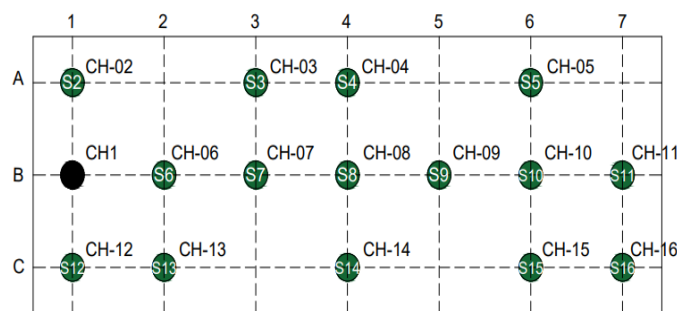


Fig. 3 Schematic diagram of the location of the accelerometer

The accelerometers were represented by the green dot while the black dot represents a location where the hammer was impacted. An impact hammer was used as a vibration excitor while accelerometers were used to record and measure the vibration wave. Each of the accelerometers was connected to the data logger using cables. The connection of the accelerometers to the data logger was according to the number of channels as shown in Figure 4 (a). Then, the data logger was connected to the computer so that the vibration wave could be recorded. Figure 4 (b) shows the hammer that was used in the impact hammer test.



Fig. 4 Laboratory testing (a) Impact hammer test equipment; (b) Four-point bending test

The impact hammer test was first done on the uncracked concrete slab where there was no load applied on the slab. The impact hammer hit point B1 as shown in Figure 5 ten times. Then, the wave vibration would be measured by the accelerometer and transferred to the computer by the data logger. The frequency response functions (FRFs) sent by the data logger would be processed by the ME'scope software installed in the computer. Static load from the four-point bending test was applied as shown in Figure 4 (b) after the impact hammer test was done on the uncracked slab. Under the four-point bending test, the slab was put under the load until the first crack occurred. The impact hammer was then hit once again at point B1 ten times. The accelerometers measured the vibration waves and sent them to the computer through the data logger. The load was then increased to get a second crack. The impact hammer test was done to see the frequency difference of the vibration waves when the crack on the slab increased. Finally, the difference in frequency between the uncracked and cracked slabs was evaluated.

The crack depth measurement was conducted by arranging the accelerometers along the crack line as shown in Figure 5 and an impact hammer test was conducted. The blue dotted lines shown in Figure 8 represent new gridlines constructed on the slab to place the accelerometers.

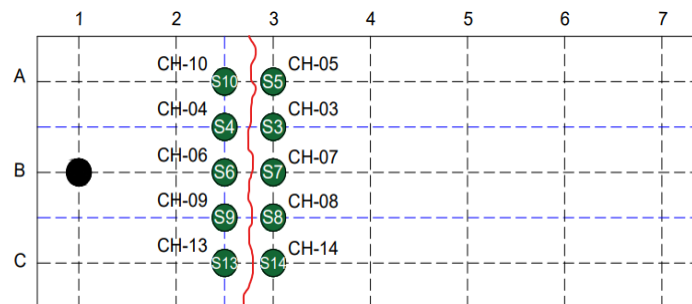


Fig. 5 Arrangement of accelerometers along the crack line

Each hammer excitation produced peak acceleration. Therefore, the acceleration of the vibration wave at each channel for both slabs was obtained by calculating the average of ten peak accelerations since there were ten excitations of the hammer on the slabs. As shown in Figure 8 accelerometers S10, S4, S6, S9 and S13 indicate the acceleration on the left side of the crack line. Meanwhile, acceleration S5, S3, S7, S8 and S14 indicate the acceleration on the right side of the crack line. The purpose of placing the accelerometer at both sides of the crack line.

4. Results and Discussion

4.1 Crack Mapping

The pattern and location of the cracking for both Slab 1 and Slab 2 were almost the same as shown in Figure 9 and Figure 10. The slab was loaded for 3 kN and 6 kN, 12 kN and 15 kN. However, there was no result for the 3 kN and 6 kN loads because the load was automatically set up to 12 kN from the machine during the four-point bending test, and the machine only stopped when the load reached 12 kN. Meanwhile, for Slab 2, the four-point bending test was performed by gradually increasing the load from 3 kN to 6 kN, 12 kN, and 15 kN. However, no cracking was observed during the 3 kN and 6 kN loading. Only after applying 12 kN and 15 kN loads did the flexural crack

appear at the middle of the slab. The bending of the slab created a tensile stress that exceeded the tensile strength of the concrete, which resulted in a flexural crack.



Fig. 5 Crack mapping (a) slab 1; (b) slab 2

4.2 Natural Frequency

The data collected during the impact hammer test was then analysed in the Me'Scope software package. The raw data was transformed into the Fast Fourier Transform (FFT) function as illustrated in Figures 5 (a) and (b), and Figure 6 to display the natural frequency of the vibration waves. The natural frequency of the slabs before and after crack is shown in Table 1.

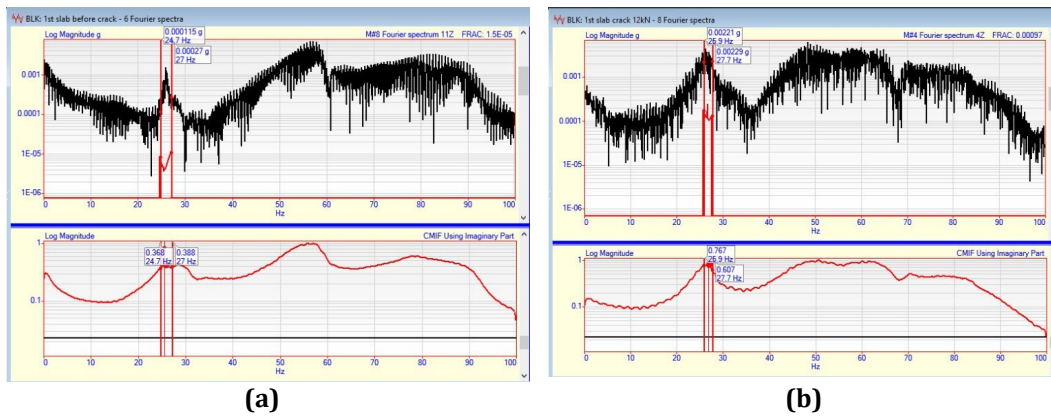


Fig. 5 Fourier transform of slab 1 (a) Before crack; (b) 12 kN load

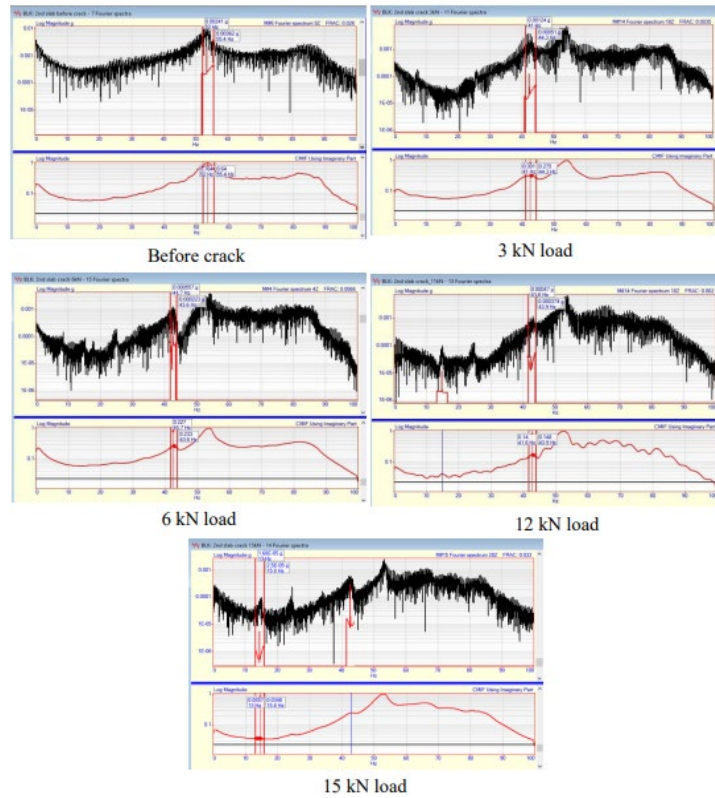


Fig. 6 Fourier spectrum of slab 2

The result shown in Table 1 described that the natural frequency of slab 1 and slab 2 decreased after the crack compared to before the crack. In Slab 2, the natural frequency decreases more noticeably at 12 kN and 15 kN as crack development increases. Reduced in the natural frequency was anticipated due to the decrease in the stiffness following the crack [21] and [22].

Table 1 Natural frequency of slabs before and after crack

		Natural frequency (Hz)				
		Before crack	After crack			
			3 kN load	6 kN load	12 kN load	15 kN load
Slab 1	25.6	NA	NA	14.6	NA	
Slab 2	27.1	24.9	24.5	14.8	9.3	

4.3 Crack Depth Measurement

The acceleration along the crack was compared to understand the crack width of the slab. Figure 13 show the graph of acceleration against time in second for the impact hammer test. Ten vibration waves indicate that the hammer was hit ten times on the slab. The acceleration is represented by the y-axis of the graph. Figure 14 shows the peak acceleration of the vibration waves.

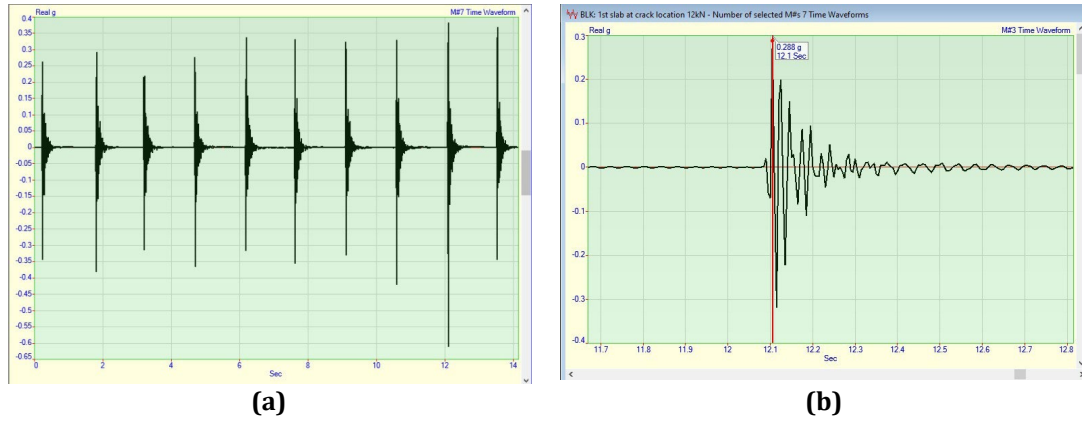


Fig. 7 Analysis result of (a) Vibration wave of slab 1 at 12 kN; (b) Peak acceleration of vibration wave

Table 2 Acceleration of vibration waves at slab 1

Load (kN)	Point	Acceleration (g)				Percentage difference (%)
		Left side		Right side		
12	NA	CH 10	NA	CH 5	NA	NA
	NA	CH 4	NA	CH 3	0.2540	NA
	3	CH 6	0.1774	CH 7	0.3134	13.6
	2	CH 9	0.2101	CH 8	0.3189	10.88
	1	CH 13	0.2310	CH 14	0.3271	9.61

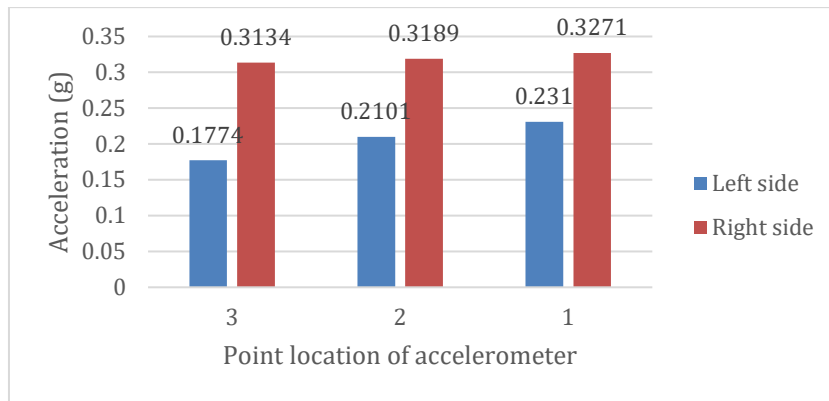


Fig. 8 Acceleration of the wave on slab 1 from left to right after propagating through the crack area

Due to unstable vibration waves from the impact hammer test, acceleration data for CH-10, CH-5, and CH-4 could not be acquired. Therefore, the acceleration of the vibration wave is only compared for points 1, 2 and 3 only. As a result, the highest acceleration was unknown. Table 2 and Figure 8 show that after the wave propagate through the crack area, a noticeable acceleration increment was observed in a left-to-right direction. The increase in acceleration signifies a change in the magnitude or intensity of the wave as it transverse the crack. As the acceleration decreased from point 1 to point 3, the percentage difference between the accelerations increased. By comparing the percentage difference at points 1, 2 and 3, the highest percentage difference was at point 3. Meanwhile, the lowest percentage difference was at point 1.

Table 3 Crack depth on slab 1

Point	b (mm)	t1 (mm)	t2 (mm)	Crack depth (mm)
1	0	81.4	149.5	51
2	100	110.3	209	40
3	200	108.3	204	42
4	500	71.8	141.3	21
5	600	82.1	144.2	66

The result was compared with the measurement of crack depth using PUNDIT. Table 3 shows the result of PUNDIT for Slab 1. From Table 3, the crack depth at point 1 was 51 mm which was the highest compared to the crack depth at point 2 and point 3.

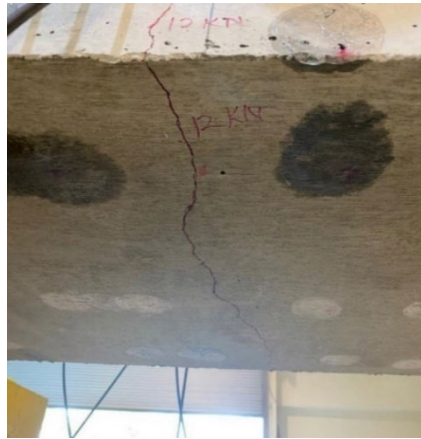


Fig. 9 Size of crack on slab 1

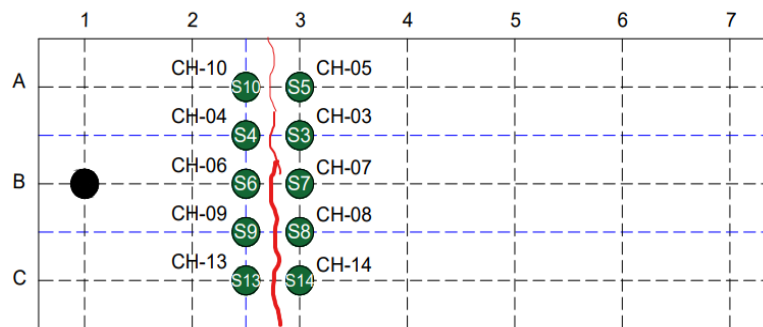


Fig. 10 Sketch of the crack width on slab 1

Figure 9 shows the size of the crack on Slab 1 and Figure 10 shows the sketch of the crack size on Slab 1. It was observed during the testing that the width of the crack was larger around gridline C to B at point 1. Therefore, it can be justified that at point 1, the crack depth and crack width were the highest. It also can be justified that when the percentage difference of the acceleration decreased, the crack width increased.

Table 4 Acceleration of vibration waves at slab 2

Load (kN)	Point	Acceleration (g)				Percentage difference (%)
		Left side		Right side		
12	5	CH 10	0.2513	CH 5	0.3069	5.56
	4	CH 4	0.2471	CH 3	0.3238	7.67
	3	CH 6	0.2571	CH 7	0.3459	8.88
	2	CH 9	0.2906	CH 8	0.31	1.94
	1	CH 13	0.2592	CH 14	0.3198	6.06

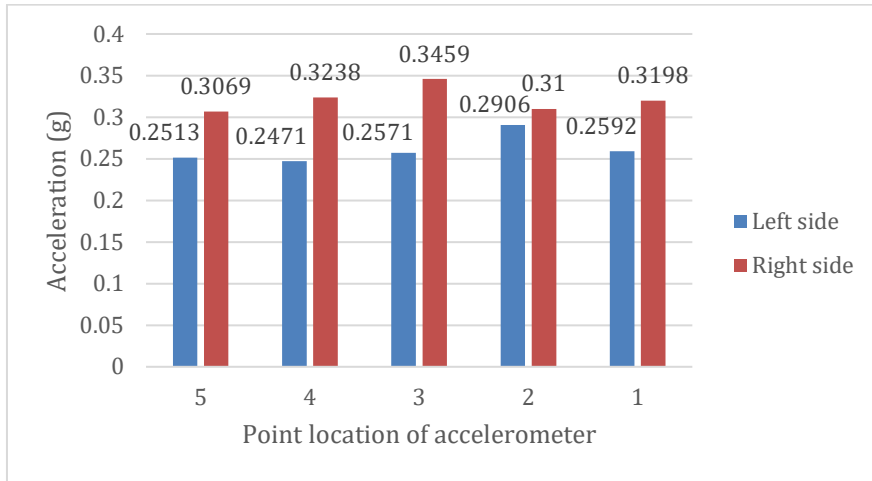


Fig. 11 Acceleration of the wave on slab 2 from left to right after propagating through the crack area

The wave acceleration increased from the left to the right side, as shown in Table 4 and Figure 18. The highest percentage difference was at point 3 while the lowest percentage difference was at point 2.

Table 5 Crack depth on slab 2

Point	b (mm)	t1 (mm)	t2 (mm)	Crack depth (mm)
1	0	72.3	125.5	70
2	100	104.7	151.1	133
4	500	153.6	247	94
5	600	74.3	124	82

The result was compared with the measurement of crack depth using PUNDIT. Table 5 shows the result of PUNDIT for Slab 2. A crack depth reading for point 3 could not be acquired due to safety factors as point 3 was located under the slab. From Table 5, the highest crack depth was 133 mm which appeared at point 2.

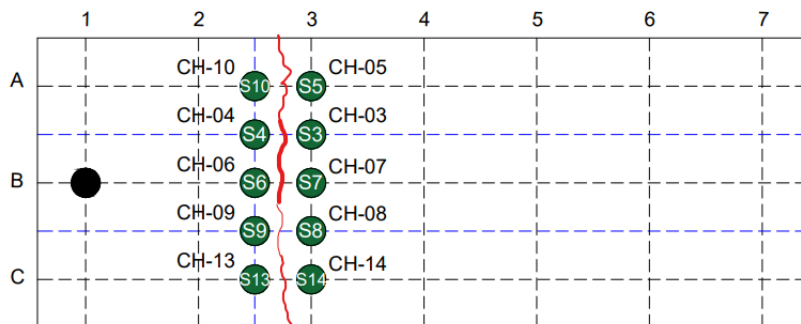


Fig 12 Sketch of the crack width on slab 2

Figure 12 depicts the size of the crack on Slab 2 complying with the result from the impact hammer test and PUNDIT. During the testing, it was observed that the widest crack width was located at point 2. Therefore, it can be justified that at point 2, the crack depth and crack width were maximum. It also can be justified that when the percentage difference of the acceleration decreased, the crack width increased.

From the overall result of the crack width measurement, it can be concluded that the percentage difference in the waves' acceleration was inversely proportional to the crack width. When the percentage difference of the acceleration was decreased, the crack width increased. The result was validated with the comparison to the crack depth measurement. The result of the crack depth measurement showed that the location of the maximum crack depth was the same as the maximum crack width. However, crack width assessment using an impact hammer test had not been discussed yet in any previous study. Therefore, further research needs to be performed to understand the propagation of the waves through the crack area so that the findings of this study can be validated.

5. Conclusion

In this study, an impact hammer test has been carried out to find the natural frequency of cracked and uncracked slabs as well as to determine the width of the crack. The natural frequency of both Slab 1 and Slab 2 was lower after the crack than it was before the crack. The findings validated a previous study that found that the natural frequency after cracking was lower than it was before cracking due to the reduced stiffness after cracking. For crack width measurement, after propagating through the crack region, it was discovered that the wave's acceleration increased. The percentage difference of the waves' acceleration from left to right after the wave propagated through the crack area was calculated to determine the width of the crack. The result shows that when the percentage difference decreased, the width of the crack increased. The findings were proved by comparing the data with crack depth measurement using PUNDIT. From the comparison, it can be observed that the location of maximum crack depth and crack width was the same. However, further research needs to be done to prove this finding on the measurement of crack width using an impact hammer test.

Acknowledgement

The authors would like to thank the supervisor, family and friends for their help and support in completing this research. The author also would like to thank the Faculty of Civil Engineering and Built Environment, Universiti Tun Hussein Onn Malaysia for making this happen.

References

- [1] Yao, Y., Tung, S. T. E., & Glisic, B. (2014, December 1). Crack detection and characterization techniques - An overview. *Structural Control and Health Monitoring*, Vol. 21, pp. 1387–1413.
- [2] Issa, C. A., & Debs, P. (2007). Experimental study of epoxy repairing of cracks in concrete. *Construction and Building Materials*, 21(1), 157–163.
- [3] Mohan, A., & Poobal, S. (2018). Crack detection using image processing: A critical review and analysis. *Alexandria Engineering Journal*, 57(2), 787–798.
- [4] Wu, R. T., & Jahanshahi, M. R. (2020, March 1). Data fusion approaches for structural health monitoring and system identification: Past, present, and future. *Structural Health Monitoring*, Vol. 19, pp. 552–586.
- [5] Capozucca, R. (2013). A reflection on the application of vibration tests for the assessment of cracking in PRC/RC beams. *Engineering Structures*, 48, 508–518.
- [6] Pan, J., Zhang, Z., Wu, J., Ramakrishnan, K. R., & Singh, H. K. (2019). A novel method of vibration modes selection for improving accuracy of frequency-based damage detection. *Composites Part B: Engineering*, 159, 437–446.
- [7] Brownjohn, J. M. W., de Stefano, A., Xu, Y. L., Wenzel, H., & Aktan, A. E. (2011). Vibration-based monitoring of civil infrastructure: Challenges and successes. *Journal of Civil Structural Health Monitoring*, 1(3–4), 79–95.
- [8] Farrar, C. R., & Worden, K. (2007). An introduction to structural health monitoring. *Philosophical Transactions of the Royal Society A: Mathematical, Physical and Engineering Sciences*, 365(1851), 303–315.
- [9] Ferreira, G. S., Pimentel, R. L., & Barbosa, F. de S. (2020). Evaluation of two crack models for reinforced concrete one-way slabs subjected to bending by means of modal tests. *Structures*, 28, 2013–2022.
- [10] Döhler, M., Hille, F., & Mevel, L. (2018). Vibration-based monitoring of civil structures with subspace-based damage detection. *Intelligent Systems, Control and Automation: Science and Engineering*, 92, 307–326.
- [11] Das, S., Saha, P., & Patro, S. K. (2016). Vibration-based damage detection techniques used for health monitoring of structures: a review. *Journal of Civil Structural Health Monitoring*, 6(3), 477–507.
- [12] Fan, W., & Qiao, P. (2011, January). Vibration-based damage identification methods: A review and comparative study. *Structural Health Monitoring*, Vol. 10, pp. 83–111.
- [13] Yang, Y., Zhang, Y., & Tan, X. (2021). Review on vibration-based structural health monitoring techniques and technical codes. *Symmetry*, 13(11).
- [14] Ooijevaar, T. H., Warnet, L. L., Loendersloot, R., Akkerman, R., & Tinga, T. (2016). Impact damage identification in composite skin-stiffener structures based on modal curvatures. *Structural Control and Health Monitoring*, 23(2), 198–217.
- [15] Aguilar, R., Ramírez, E., Haach, V. G., & Pando, M. A. (2016). Vibration-based nondestructive testing as a practical tool for rapid concrete quality control. *Construction and Building Materials*, 104, 181–190.
- [16] Pereira, S., Magalhães, F., Gomes, J. P., Cunha, Á., & Lemos, J. V. (2021). Vibration-based damage detection of a concrete arch dam. *Engineering Structures*, 235.
- [17] Shatilov, Y. Y., & Lyapin, A. A. (2018). Vibration-based damage detection techniques for health monitoring of construction of a multi-storey building. *Materials Science Forum*, 931 MSF, 178–183.
- [18] Altunışık, A. C., Okur, F. Y., Karaca, S., & Kahya, V. (2019). Vibration-based damage detection in beam structures with multiple cracks: modal curvature vs. modal flexibility methods. *Nondestructive Testing and Evaluation*, 34(1), 33–53.

- [19] Chinka, S. S. B., Putti, S. R., & Adavi, B. K. (2021). Modal testing and evaluation of cracks on cantilever beam using mode shape curvatures and natural frequencies. *Structures*, 32, 1386–1397.
- [20] Pimentel, R., Guedes, T., Melo, L., Ferreira, G., & Gonçalves, M. (2017). Damage detection assessment in reinforced concrete slabs using impact tests. *Procedia Engineering*, 199, 1976–1981.
- [21] Daves, M., Ervin, E. K., & Zeng, C. (2021). Experimental data interpretation using genetic algorithm for global health assessment of reinforced concrete slabs subjected to cracking. *Advances in Structural Engineering*, 24(3), 411–421
- [22] Hashim, H., Ibrahim, Z., & Razak, H. A. (2013). Dynamic characteristics and model updating of damaged slab from ambient vibration measurements. *Measurement: Journal of the International Measurement Confederation*, 46(4), 1371–1378.